



Thermal Performance of a Double-Pass Solar Air Heater

Roonak Daghigh* , Abdellah Shafieian

Department of Mechanical Engineering, University of Kurdistan, Sanandaj, Kurdistan, Iran

PAPER INFO

Paper history:

Received 15 October 2015

Accepted in revised form 03 May 2016

Keywords:

Double-pass absorber
Solar air heater
Building heating
Sanandaj

ABSTRACT

This study analyzes the thermal performance of solar thermal energy using double-pass absorber plate in Sanandaj, Iran. To this end, a mathematical model was encoded according to the energy and exergy balance equations and solved by MATLAB software. Given the environmental conditions and radiation intensity of a winter day in Sanandaj, the effects of external parameters such as radiation intensity and internal parameters like canal's height, inlet mass flow rate, absorber length as well as some physical parameters on the efficiency of the system were analyzed and the energy and exergy output of the system was studied. To validate the proposed model, the results obtained from numerical simulation were compared with experimental data, which showed an acceptable compatibility. Finally, the ability of the system to supply the thermal load of the building in the given day was examined and the roles of various factors in the area under thermal coverage of this system were analyzed. The obtained findings indicated that a system with an area of 3 m² and mass rate of 250 kg/h in radiation intensity of 619 W/m² and temperature of 3.45° is capable of supplying the thermal load of a space with an approximate area of 14 m.

1. INTRODUCTION

Solar energy is one of the most significant sources of renewable energies. The radiation rate of solar energy at various areas around the world is variable and the solar belt of the earth contains the highest amount of solar energy. Iran is also located in a high radiation zone. Studies have shown that the application of solar facilities in Iran is appropriate and can supply part of the energy required in the country. According to the experts, Iran with 300 sunny days in more than two third of it and average radiation of 4.5-5.5 kWh/m²/day has been introduced as one of the countries with high potential in solar energy [1].

Buildings consume more than one third of the energy in Iran. Heating systems are the biggest consumers of energy in the buildings so that about 57% of energy is

devoted to providing heating and cooling in a building. Since a great amount of energy is consumed in buildings and fossil fuels are increasingly decreased, it is necessary to take justifiable and quicker measures to help with solving this problem .

The idea of using double-pass air heaters with countercurrent flow was first introduced by Satcunanathan and Deonarine [2]. The air is first flown between the glass space and absorber plate and then through the lower canal. Using such a system can reduce the thermal loss through application of one or more glass covers [3]. Wijeysondera et al compared a two-pass heating transfer model with a one-pass heating transfer system. The simulation results showed that open systems with intake fluid at environment temperature are 10-15% more efficient than one-pass systems . Another mathematical model was developed by Persad and Satcunanathan to predict the performance of double glazed glass under one-pass and double-pass conditions. The results of their study revealed that the performance of two-pass system is independent of the

*Corresponding author: r.daghigh@uok.ac.ir; daghighm@gmail.com
(R. Daghigh)

collector's length, and the degree of glass cover heat depends on the distance between plates [4].

Various double-pass air heaters have been introduced to increase the heat transfer rate, which leads to improvement of thermal performance. These techniques result in an increase in heat transfer between the absorber plate and air, which clearly leads to enhancement of the thermal performance of solar collector [5, 6]. Sopian et al conducted an experimental study on a two-pass solar collector with and without porous coatings on the second channel [7]. The collector had only a glass cover and a black metal absorber, and the material used was a porous coating of steel wool. Krishnananth et al investigated a two-pass solar collector with thermal storage [8]. Paraffin wax was used as a thermal collector and its performance was studied for different structural plans. Alkilani et al showed that it is possible to enhance thermal output to 18% by a usual two-pass collector than by a usual air heater [9].

So far, numerous studies have been carried out about the design, simulation and optimization of different solar air thermal systems [10-13]. These systems are classified into active and inactive groups. In inactive systems like Trombe wall [14] and solar windows [15], solar energy is used with no mobile instrument; whereas, in active systems, a mechanical device is used to distribute the absorbed energy [16]. Nevertheless, both methods have problems of their own. Inactive solar heating is limited to the rooms with a sunny slope and active solar heating is costly [17]. Bansal [18] studied the application of solar air heaters and their performance parameters in India.

It has been proven that an exergy study (or second law study) is a useful tool in analysis of energy systems. Estimating quantitatively the sources of the thermodynamic imperfection, is the duty of exergy analyses [19, 20]. Akpınar et al. experimentally studied the performance of a new flat-plate solar air heater with and without obstacles on the absorber plates. Energy and exergy relationships for this new flat-plate solar air heater and for different solar air heaters were calculated [21]. Bouadila et al. designed a solar air heater with a packed-bed latent storage energy system applying phase change materials and investigated energy and exergy efficiency. [22]. It has been proven that the highest exergy destruction (irreversibility) in solar systems for building applications, occurs in the solar collector. The daily energy and exergy efficiency of solar collector varies between 25%-65% and 1%-3.5% respectively [23]. Energy and exergy performance evaluation of solar air heaters with inserted porous baffles was conducted by Bayrak et al. [24]. The obtained results showed that the highest temperature difference is achieved in air mass flow rate of 0.025 kg/s. Although numerous energy analyses have been conducted of solar systems, the number of papers which consider exergy

analysis is very limited.

In the present study, the thermal performance of solar air heating system and the effect of different parameters on it were analyzed through a simulated numerical method in a winter day in Sanandaj, Iran. The main purpose of proposed system is supplying whole or a part of the thermal load of a space. So, the ability of this system to supply the thermal load with specific characteristics in Sanandaj was investigated and the role of various factors affecting the area under the thermal coverage of this system was analyzed.

2. NUMERICAL SIMULATION

2-1. Double Pass Solar Collector

A mathematical model based on energy balance was established (Fig. 1). This model consists of balance equations at glass cover, air flow, absorber and plates.

The following assumptions are considered in this study [25]:

- Capacity effects of glass cover, absorber plate are not considered.
- The temperature of glass cover, plates and air flow vary in the x direction.
- Side heat losses are neglected.
- Air leakage is not considered.

Air is considered as an ideal gas with constant heat capacity.

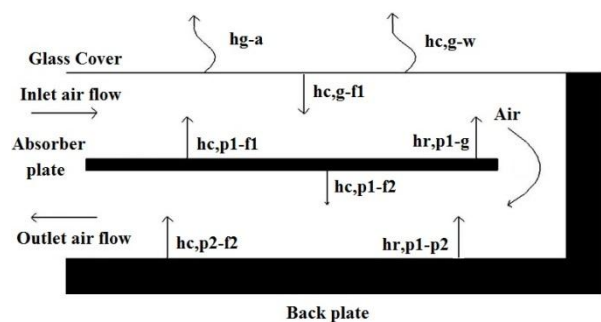


Figure 1. Schematic of double pass collector

Energy balance for the double pass system is as follows
 Glass cover All glass covers absorb a percentage of sun light. Absorbed energy is that part of radiation which is not transmitted through the glass or reflected off of its surface. Absorbed energy will be converted to heat, which increases the glass temperature [26].

$$\alpha_g S_g = h_{r,g-a}(T_g - T_a) + h_{c,g-w}(T_g - T_w) + h_{r,p-g}(T_g - T_p) + h_{c,g-f1}(T_g - T_{f1}) \quad (1)$$

$$h_{r,p1-p2}(T_{p1} - T_{p2}) + h_{c,p2-f2}(T_{f2} - T_{p2}) = U_r(T_{p2} - T_a) \quad (5)$$

Flowing air between glass cover and absorber

$$h_{c,r1-g}(T_g - T_{r1}) = \frac{\dot{m} C_f}{B} \frac{dT_{r1}}{dX} + h_{c,p1-r1}(T_{r1} - T_{p1}) \quad (2)$$

Absorber plate

$$\tau_g \tau_p S_a + h_{r,p-a}(T_g - T_a) = h_{r,p-f1}(T_{f1} - T_p) + h_{c,p-f1}(T_{f1} - T_p) + h_{r,p-f2}(T_{f2} - T_p) \quad (3)$$

In order to rewrite the mentioned equation in the terms of flowing air temperature, equations 1, 3 and 5, are substituted in equations 2 and 4. The following two linear first-order differential equations are obtained.

$$\frac{dT_{r1}}{dX} = \gamma_1 T_{r1} + \gamma_2 T_{r2} + C_1 \quad (6)$$

Flowing air between two plates

$$(4) h_{c,p1-f2}(T_{p1} - T_{f2}) = -\frac{\dot{m} C_f}{B} \frac{dT_{f2}}{dX} + h_{c,p2-f2}(T_{f2} - T_{p2}) \quad (4)$$

$$\frac{dT_{f2}}{dX} = \beta_1 T_{r1} + \beta_2 T_{r2} + C_2 \quad (7)$$

For the back plate

$$\gamma_1 = \frac{\left(\frac{h_{c,f1-g} h_{r,p1-g}}{k} + h_{c,p1-f1} \right) \left[\frac{-B h_{c,f1-g} h_{r,p1-g} - b B h_{c,p1-f1} \left(\frac{U_r + h_{c,p1-f2} + h_{r,p1-p2}}{h_{r,p1-p2}} \right)}{\dot{m} C_f} \right]}{\left(\frac{h_{r,p1-g}^2}{k} - h_{r,p1-g} \right) \left(\frac{U_r}{h_{r,p1-p2}} + \frac{h_{c,p1-f1}}{h_{r,p1-p2}} + 1 \right) - \left(\frac{U_r}{h_{r,p1-p2}} + \frac{h_{c,p1-f1}}{h_{r,p1-p2}} \right) (h_{r,p1-p2} + h_{c,p1-f1} + h_{c,p1-f2}) - (h_{c,p1-f1} + h_{c,p1-f2})} + \frac{B h_{c,f1-g} (h_{c,f1-g} - 1)}{b \dot{m} C_f} - \frac{B h_{c,p1-f1}}{\dot{m} C_f} \quad (8)$$

$$\gamma_2 = \frac{\left[\frac{h_{r,p1-g} h_{c,p2-f2}}{h_{r,p1-p2}} \left(1 - \frac{h_{r,p1-g}}{k} \right) + \frac{h_{c,p2-f2}}{h_{r,p1-p2}} (h_{r,p1-p2} + h_{c,p1-f1} + h_{c,p1-f2}) + h_{c,p1-f2} \right] \left[\frac{B h_{c,f1-g} h_{r,p1-g}}{k \dot{m} C_f} \left(\frac{U_r + h_{c,p1-f2} + h_{r,p1-p2}}{h_{r,p1-p2}} \right) \right]}{\left(\frac{h_{r,p1-g}^2}{k} - h_{r,p1-g} \right) \left(\frac{U_r}{h_{r,p1-p2}} + \frac{h_{c,p1-f1}}{h_{r,p1-p2}} + 1 \right) - \left(\frac{U_r}{h_{r,p1-p2}} + \frac{h_{c,p1-f1}}{h_{r,p1-p2}} \right) (h_{r,p1-p2} + h_{c,p1-f1} + h_{c,p1-f2}) - (h_{c,p1-f1} + h_{c,p1-f2})} - \frac{B h_{c,p1-f1} h_{c,p2-f2}}{\dot{m} C_f h_{r,p1-p2}} \quad (9)$$

$$\beta_1 = \frac{\left(\frac{h_{c,f1-g} h_{r,p1-g}}{k} + h_{c,p1-f1} \right) \left[\frac{B h_{c,p2-f2} + B h_{c,p1-f2} \left(\frac{U_r + h_{c,p1-f2} + h_{r,p1-p2}}{h_{r,p1-p2}} \right)}{\dot{m} C_f} \right]}{\left(\frac{h_{r,p1-g}^2}{k} - h_{r,p1-g} \right) \left(\frac{U_r}{h_{r,p1-p2}} + \frac{h_{c,p1-f1}}{h_{r,p1-p2}} + 1 \right) - \left(\frac{U_r}{h_{r,p1-p2}} + \frac{h_{c,p1-f1}}{h_{r,p1-p2}} \right) (h_{r,p1-p2} + h_{c,p1-f1} + h_{c,p1-f2}) - (h_{c,p1-f1} + h_{c,p1-f2})} \quad (10)$$

$$\beta_2 = \frac{\left[\frac{h_{r,p1-g} h_{c,p2-f2}}{h_{r,p1-p2}} \left(1 - \frac{h_{r,p1-g}}{k} \right) + \frac{h_{c,p2-f2}}{h_{r,p1-p2}} (h_{r,p1-p2} + h_{c,p1-f1} + h_{c,p1-f2}) + h_{c,p1-f2} \right] \left[\frac{B h_{c,p2-f2} - B h_{c,p1-f2} \left(\frac{U_r + h_{c,p1-f2} + h_{r,p1-p2}}{h_{r,p1-p2}} \right)}{\dot{m} C_f} \right]}{\left(\frac{h_{r,p1-g}^2}{k} - h_{r,p1-g} \right) \left(\frac{U_r}{h_{r,p1-p2}} + \frac{h_{c,p1-f1}}{h_{r,p1-p2}} + 1 \right) - \left(\frac{U_r}{h_{r,p1-p2}} + \frac{h_{c,p1-f1}}{h_{r,p1-p2}} \right) (h_{r,p1-p2} + h_{c,p1-f1} + h_{c,p1-f2}) - (h_{c,p1-f1} + h_{c,p1-f2})} + \frac{B h_{c,p1-f2} h_{c,p2-f2}}{\dot{m} C_f h_{r,p1-p2}} \quad (11)$$

Equations 6 and 7 can be solved by numerical methods. But, another solution method is applied in this study. Firstly, equations 6 and 7 are combined as follows:

$$\frac{d(T_{f1} + \lambda_2 T_{f2})}{dx} = C(T_{f1} + \lambda_2 T_{f2}) + K \quad (12)$$

$$C = \gamma_1 + \lambda_2 \beta_1 \quad (13)$$

$$\lambda_2 = \frac{\gamma_2 + \lambda_2 \beta_1}{\gamma_1 + \lambda_2 \beta_1} \quad (14)$$

$$K = C_1 + \lambda_2 C_2 \quad (15)$$

$$T_{f1} + \lambda_2 T_{f2} = -\frac{K}{C} + \frac{B}{C} e^{Cx} \quad (16)$$

$$T_{f1} + \lambda_{21} T_{f2} = -\frac{K_{11}}{C_{11}} + \frac{B_{11}}{C_{11}} e^{C_{11}x} \quad (17)$$

$$T_{f1} + \lambda_{21} T_{f2} = -\frac{K_{22}}{C_{22}} + \frac{B_{22}}{C_{22}} e^{C_{22}x} \quad (18)$$

The constants B11 and B22 are determined using following boundary conditions:

$$\begin{aligned} T_{f1}(x=0) &= T_a \\ T_{f1}(x=L) &= T_{f2}(x=L) \end{aligned}$$

The forced convective heat transfer coefficients are calculated by [27]:

$$h = 0.0158 (Re^{0.8}) \frac{k}{D_h} \quad (19)$$

$h_{r,gs}$ and $h_{c,gw}$ form the overall heat transfer coefficient from the glass to the ambient and takes the value of 25 w/m²K. In order to obtain the temperature distribution of flowing air inside collector, mentioned equations are solved using MATLAB computer program.

2.2. Exergy Efficiency

The analysis assumptions in this study are [21]:

- Equations are developed under steady state and steady flow.
- Potential and kinetic energy effects are neglected and there is no chemical or nuclear reactions.
- Air is considered as an ideal gas, so has a constant specific heat.
- The directions of heat transfer to the system are considered positive.

Exergy balance equation is applied to achieve exergy efficiency [23].

$$\sum \dot{E}x_{in} - \sum \dot{E}x_{out} = \sum \dot{E}x_{dest} \quad (20)$$

$$\dot{E}x_{heat} - \dot{E}x_{work} + \dot{E}x_{mass,in} - \dot{E}x_{mass,out} = \dot{E}x_{dest} \quad (21)$$

It can also be written as:

$$\sum \left(1 - \frac{T_0}{T_k}\right) Q_k - W + \sum \dot{m}_{in} \psi_{in} - \sum \dot{m}_{out} \psi_{out} = \dot{E}x_{dest} \quad (22)$$

is flow exergy and can be calculated by:

$$\psi = (h - h_0) - T_0(s - s_0) \quad (23)$$

Exergy efficiency can be defined as the ratio of useful delivered exergy to the absorbed exergy by the solar collector [28].

$$\eta_{sc} = \frac{\dot{E}x_u}{\dot{E}x_{sc}} \quad (24)$$

$$\dot{E}x_u = \dot{m}_w [(h_o - h_i) - T_0(s_o - s_i)] \quad (25)$$

$$\dot{E}x_u = \dot{m} C_w \left[(T_o - T_i) - T_0 \left(\ln \frac{T_o}{T_i} \right) \right] \quad (26)$$

$$\dot{E}x_{sc} = A I_T \left[1 + \frac{1}{3} \left(\frac{T_0}{T_{sr}} \right)^4 - \frac{4}{3} \left(\frac{T_0}{T_{sr}} \right) \right] \quad (27)$$

While using mentioned equation in calculating the exergy of solar radiation, solar radiation temperature, T_{sr} , is taken to be 6000 k [29].

2.3. Calculation of Thermal Load

To keep normal conditions inside a building, first the thermal load of the building is estimated and then the components of the heating system are calculated and selected, accordingly. To this end, as shown in Fig. 2, a space with a wooden door and a double glazed window with the air distance of 1.2 cm and areas of 2 and 1.5 m² on the eastern and western walls, respectively were selected in Sanandaj, Iran. Based on the statistical information about Sanandaj, the interior temperature was 23.33° C and exterior temperature was -12.77 °C. The dissipation coefficients were based on the materials of the walls and ceiling of the design location, and ventilation was performed based on the inlet fresh air and the presence of filter. Also, the southern wall was considered as an internal wall and its materials were a combination of clay brick, exterior and interior plastering and the materials of ceiling were a combination of concrete, 2.54 cm insulation and interior plastering. Based on the mentioned materials and design, the thermal dissipation coefficients for the wall, ceiling,

door and window were $0.6475\text{W/m}^2\cdot^\circ\text{C}$, $0.2275\text{W/m}^2\cdot^\circ\text{C}$, $0.7875\text{W/m}^2\cdot^\circ\text{C}$ and $1.1375\text{W/m}^2\cdot^\circ\text{C}$, respectively [19]. The temperature of 23°C and relative humidity of 45% are considered as human comfort conditions in this study.

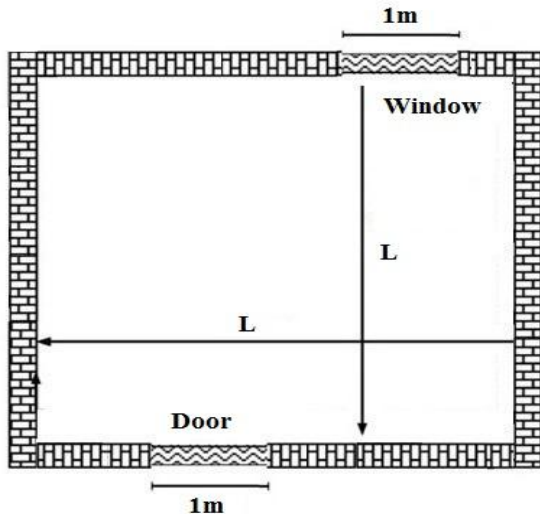


Figure 2. Spatial schematic that should be heated by solar air thermal system.

The thermal load in winter consists of two major parts:
 A: thermal loss from wall, ceiling, floor, door and window
 B: thermal loss happened as a result of the cold weather entering the building. This may occur through mandatory ventilation of the building or normal penetration of the cold air into the building through open doors, windows, etc. [20].

In calculating thermal load, the heat produced by the resources inside the building such as people and lighting systems were disregarded for the sake of assurance .

Thermal loss through the walls:

It includes all thermal transfer conducted from walls, doors, windows, ceiling and floor of the building, which was obtained via the following equation:

$$q = UA(T_{di} - T_{do}) \tag{28}$$

Where U is the total coefficient of thermal loss, T_{di} is the interior temperature and T_{do} is the exterior temperature.

Thermal loss through penetration :

To calculate thermal loss through penetration or ventilation, first the inlet air should be calculated and then volumetric method should be applied to compute the amount of thermal loss.

In this method, the following formula is used to compute the amount of inlet air:

$$V = n \times v \tag{29}$$

where V is the amount of inlet air based on ft^3/h , v is the volume of the room or the given location based on cubic feet and n is the number of times the air of the room is changed in an hour, which equals 1.5 for the rooms with two walls, a door and an outward window [30]

After calculating the volume of the air entering the room, the following equation was used to compute its thermal load :

$$q = V \times 0.0749 \times 0.241 \times (T_s - T_i) \tag{30}$$

Where V is the volume of inlet air, T_i is the interior temperature and T_s is the exterior temperature. In the above-mentioned calculations, the conditions for all the walls or 6 rooms, apart from their geographical location, were considered the same, although it is not so in reality. For instance, the southern wall of the room is warmer than the northern and eastern walls since it is more exposed to the sunshine and will have less thermal loss. Also, the rooms in upper floors have higher loss of energy than the rooms downstairs because of an increase in the air velocity.

To account these conditions, the orientation coefficients were included in calculations. In addition, 5-10 percent confidence was taken into account to make up for the computational errors for each room .

3. RESULTS

Climate and solar radiation on January 5th in Sanandaj, Iran shown in Fig. 3, were considered in calculations.

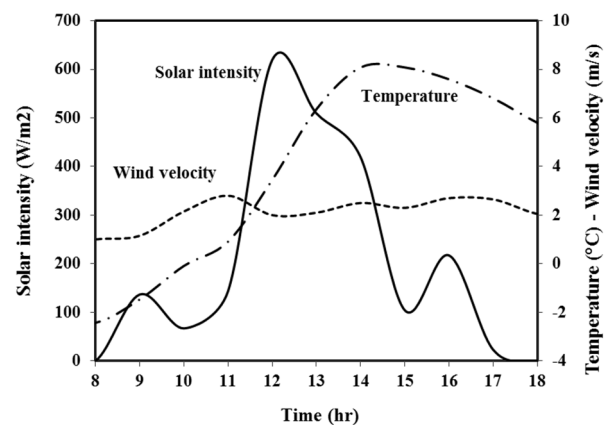


Figure 3. Climatic conditions and radiation intensity on January 5th in Sanandaj.

To analyze the effect of air distance between absorber plate and glass cover on the outlet air temperature, an absorber plate with the length of 1.5 m, width of 0.7 m and mass rate of 100 kg/h was considered for the environmental conditions at 12:00 o'clock.

At this time the radiation intensity was 619W/m^2 and temperature was 3.45°C .

Figs. 4 and 5 show the temperature at different distances for upper and lower channel .

With reduction in air distances, the outlet air temperature of the collector is dramatically increased due to the thermal loss mostly as radiation or movement which consequently leads to increment in outlet thermal load which is very favorable.

In the stable mass flow rate, the air velocity is increased along with reduction of air distance, which causes an increase in the heat transfer coefficient and consequently in outlet air temperature .

Considering the collector area, low mass flow rate and low inlet air temperature, it can not be expected that the system provides all the required thermal load and comfort conditions (like comfort temperature).

As stated, the main purpose of proposed system is supplying the whole or a part of the thermal load of a space.

Depending on different circumstances, the whole or a part of thermal load and comfort condition can be achieved. So, when the proposed system, for example provides low air temperature, can be used as a preheating system, for example, before the air enters the main heating system.

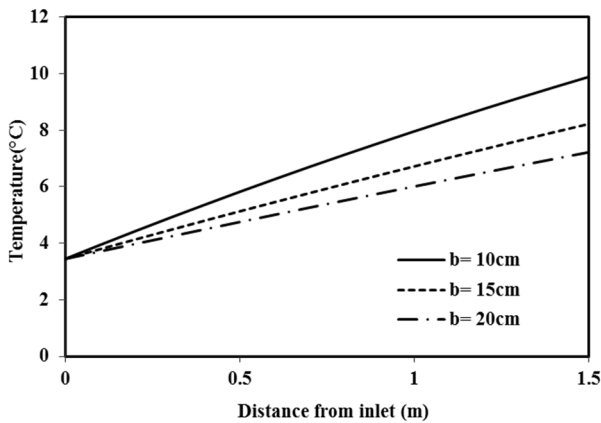


Figure 4. Outlet air temperature based on the distance from inlet with different air distances in the upper channel.

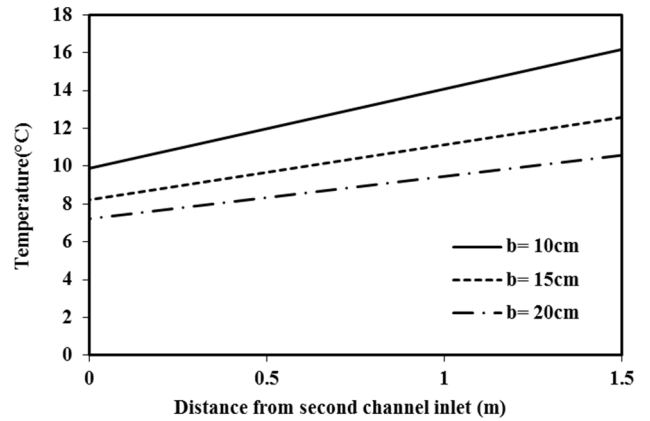


Figure 5. Outlet air temperature based on the distance from the

To analyze the effect of the mass flow rate of inlet air on outlet air temperature, the physical characteristics of the collector and environmental conditions were considered as before, the only difference, however, was that the air distance was 10 cm. Fig. 6 and 7 indicate the temperature at different distances for upper and lower channel.

Decreasing the mass flow rate of the inlet air of the collector caused an increase in the outlet air temperature and led to an increase in the output thermal load, which is very favorable. However, it should be noted that this decline in the mass flow rate reduced the output thermal load of the system.

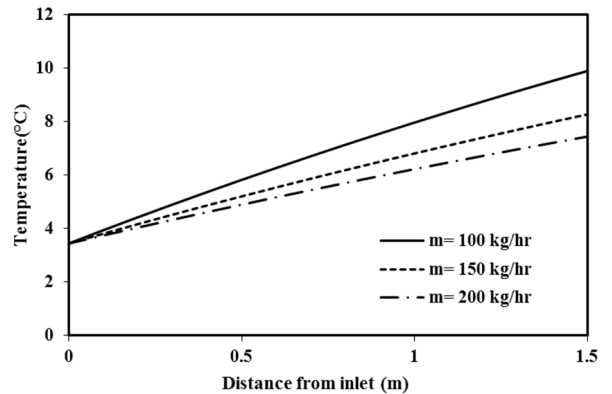


Figure 6. Outlet air temperature based on the distance from inlet with mass flow rate of inlet air in the upper channel

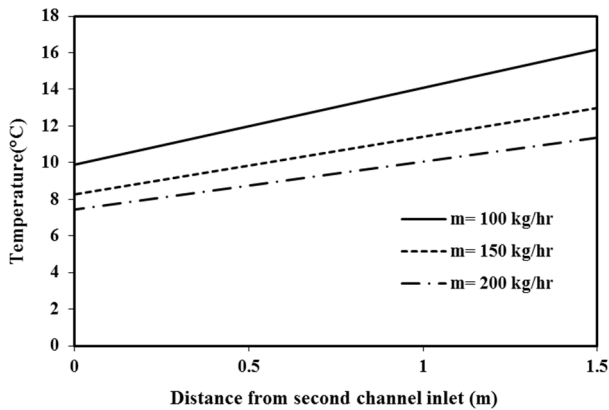


Figure 7. Outlet air temperature based on the distance from the end of the collector with mass flow rate of inlet air in the lower channel.

The thermal output of the collector is defined as the proportion of the heat transfer into the fluid to increase the temperature in radiation absorbed by the collector which is calculated by the following equation:

$$\eta = \frac{mC(T_o - T_i)}{SA} \tag{30}$$

This output is calculated for a collector with different lengths. As illustrated in fig. 8, increasing the length of collector has no significant impact on the thermal output of the collector. By increasing the length of the collector, the outlet air temperature of the collector is increased, but along with gradual increase of temperature, the heat transfer rate is reduced due to the reduction in temperature difference of the plate and passing air, which decreases the temperature changes. The refore, increasing the length of collector causes a slight increase in the output. As shown in the figure, the proportion of radiation intensity and the thermal output of collector is reverse.

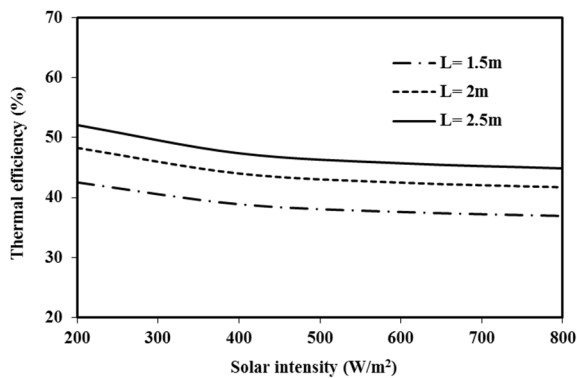


Figure 8. Thermal output of the collector based on radiation

To analyze the effect of the glass cover material on thermal output of the collector, four types of common glass covers, according to the characteristics shown in Table 1, were selected and the physical characteristics of the collector and environmental conditions were considered as the first part; the difference, however, was the 10cm distance of the air. The comparison of these four types of glass cover is illustrated in Fig. 9.

TABLE 1. Characteristics of common glass covers

| Cover Material | Thickness (mm) | Solar Transmittance |
|---------------------------|----------------|---------------------|
| Standard glass | 4 | 0.84 |
| Standard glass, tempered | 4 | 0.84 |
| Iron free glass, tempered | 4 | 0.91 |
| PMMA, ducted plate | 16 | 0.77 |

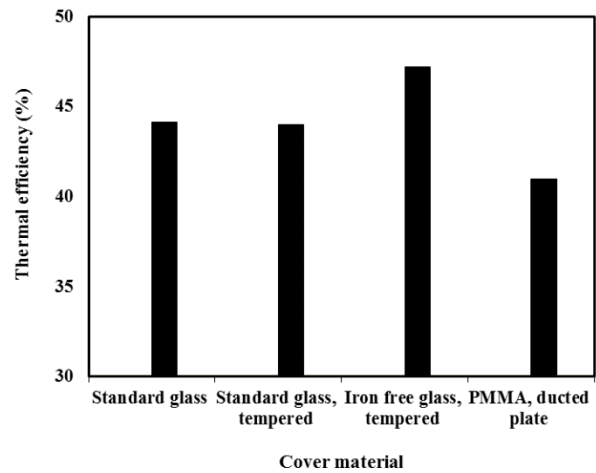


Figure 9. Effect of material used in the absorber on the thermal output of collector.

As shown in the figure, iron free tempered glass with 4 mm thickness has the optimum performance. Further, to analyze the effect of the absorber plate type on the thermal output of the collector, several absorbers with different covers, as shown in Table 2, were selected and the environmental and physical conditions were the same as the previous part. The comparison of this effect is presented in Fig. 10. As shown in the figure, the collector covered with nickel dendrites on stainless steel absorber has the best performance.

TABLE 2. Characteristics of the absorber with different

| Material | Solar normal Total Absorptivity | Emissivity at Moderate Temperature |
|-------------------------------------|---------------------------------|------------------------------------|
| CrOx on aluminum foil | 0.964 | 42 |
| CuO on aluminum sheet | 0.9 | 6 |
| NiS+ZnS on steel | 0.88 | 8.8 |
| Nickel dendrites on stainless steel | 0.99 | 3.8 |
| Zinc oxide on stainless steel | 0.95 | 11.6 |

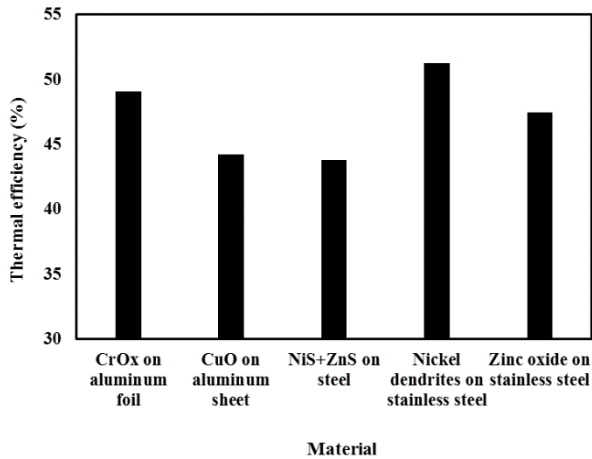


Figure 10. Effect of the material used in the absorber on thermal output of the collector.

Fig. 11, shows the thermal efficiency at different mass flow rates along the day. The effect of mass flow rate is not considerable in the beginning and at the end of the day. However, this effect becomes much more noticeable as time passes. Also, a higher efficiency is obtained at higher mass flow rates.

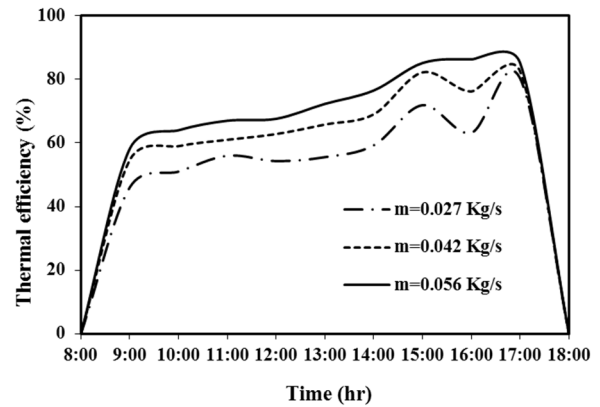


Figure 11. Thermal efficiency Vs. time.

Fig. 12, shows thermal energy supplied versus time along the day. As can be seen, there is direct relation between solar radiation and supplied energy. As time passes and solar radiation increases, supplied energy increases gradually. Maximum supplied energy happens at maximum solar radiation.

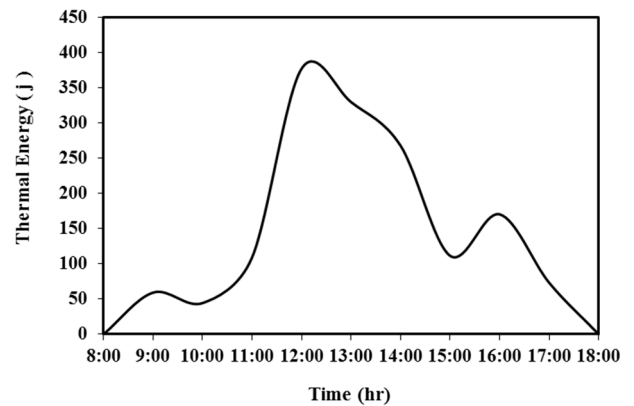


Figure 12. Thermal energy supplied vs time.

To examine the performance of this system in heating the building, a collector with an approximate area of 3 m² capable of changing the mass flow rate of the inlet air was used. Fig. 13 indicates the hourly performance of this system in thermal coverage of the given space on January 5th. As shown in this figure, radiation plays an important role in determining the thermal load supplied by the system, so that by an increase in the radiation intensity of the sun, the system can cover more area in terms of heat supply. Increasing the mass flow rate of the inlet air causes an increase in the thermal load and capability of the system. This performance difference in higher radiation intensity is more prominent. For example, take the time of 12 o'clock with radiation intensity of 619 W/m², temperature of 3.45° C and mass flow rate of 250 kg/h. As it is shown, the system is able to supply the thermal load of an approximate area of 14

m². This ability is reduced to 12.3 m² in the mass rate of 200 kg/h. To analyze the effect of collector's length, the environmental condition at 12 noon was considered. The results of the analysis presented in Fig. 14 show that increasing the length of collector or changing any parameter that causes an increase in the mass flow rate of inlet air extensively enhances the thermal application of this system.

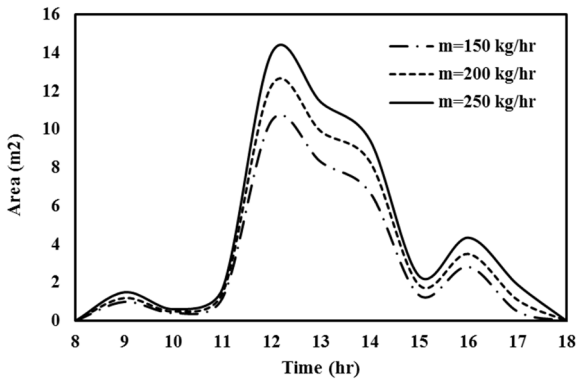


Figure 13. Effect of environmental conditions on the area under thermal coverage.

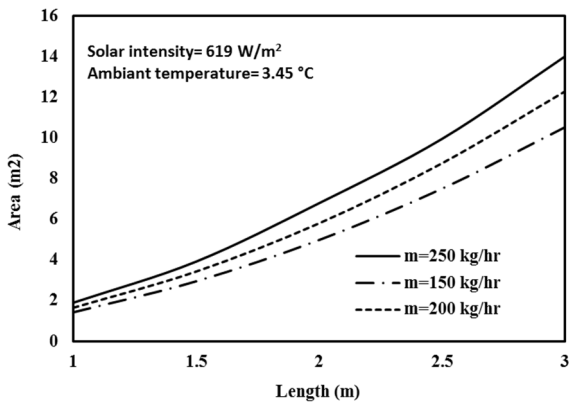


Figure 14. Effect of physical parameters on the area under thermal coverage.

Hourly exergetic analyses were performed for the proposed solar air heater collector. The length and width of the collector are 2 and 1m, respectively. The results are shown in Fig. 15. As expected, the exergy efficiency is low for the solar collector with the maximum amount of 2.2%.

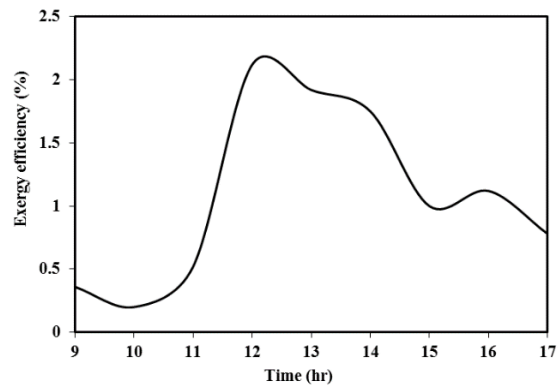


Figure 15. Exergy efficiency of solar collector vs. time.

4. VALIDATION OF SIMULATION

To validate the proposed model, the results obtained from the numerical simulation were compared with the experimental data reported by Sophian et al [31] and Naphon [32]. To this end, the environmental conditions such as radiation intensity, temperature and structural characteristics of the collector like length and width were adopted from Naphon.

The comparative results of mass flow rate of the inlet air and thermal output of the collector with a length of 2.4 m, width of 1.2 m and height of 10.5 cm and radiation intensity of 600 W/m² effects are presented in Fig. 16. Fig. 16 indicates a good agreement with maximum error of 8%. Moreover, to compare the effect of the heater's length on the outlet temperature, a collector with the same features as the collector described above with a different length was analyzed and the obtained findings were compared with experimental results. As shown in Fig. 17, these results show a good agreement with a maximum error of 6° C.

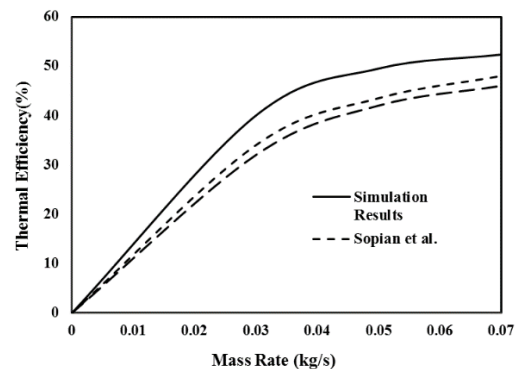


Figure 16. Comparison of the outlet air temperature obtained from numerical simulation with experimental data.

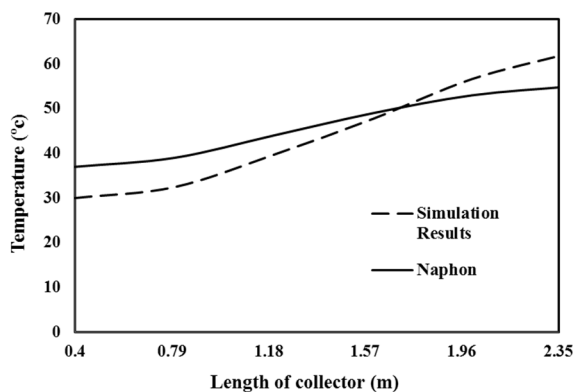


Figure 17. Comparison of the outlet air temperature obtained from numerical simulation with experimental data.

5. CONCLUSION

Cooling, heating and ventilation systems of buildings are the major energy consumers that provide the inhabitants of the buildings with thermal comfort. Solar thermal system is one of the most economical renewable technologies in which solar energy is used to heat the internal space of a building. In this study the solar thermal system was investigated through a double-pass air absorber as numerical simulation according to the climatic conditions of Sanandaj in a winter day. Findings revealed that increasing the radiation intensity augmented the temperature of the output air of the collector especially in the upper channel. This performance difference in the upper and lower channels is due to higher thermal loss as radiation and movement in the lower channel. Reduction of the channel's height significantly increased the outlet air temperature of the collector especially in the lower channel, which was followed by a rising the output thermal load. Along with reduction of air distance, the air velocity increased in the stable inlet mass flow rate, which enhanced the heat transfer coefficient followed by heat transfer increase and outlet air temperature. The decline of the mass flow rate of the collector's inlet air caused an increase in the outlet air temperature, resulting in thermal load augmentation which is quite favorable. However, it should be noted that this decline in the mass flow rate causes a decrease in the output thermal load of the system. Increasing the length of collector had little impact on the output of the collector and increased the temperature of the outlet air of the collector, but the thermal mass flow rate was declined along with gradual rise of temperature due to the decline in the temperature difference of the plate and inlet air. Iron free glass as the cover material and nickel dendrites on stainless steel as the absorber material have the optimum performance.

Furthermore, the ability of this system to supply the thermal load of the building in a cold winter day was studied. It was found out that this system has thermal cover ability for different areas, such that a system with

an area of 3 m² and mass flow rate of inlet air equal to 250 kg/h at radiation intensity of 619 W/m² and temperature of 3.45° C is able to supply the thermal load of a space with 14 m² area. The analysis of the findings showed that increasing the radiation intensity, length of collector and changing every parameter that increases the mass rate of inlet air, significantly causes an increase in the thermal application of this system. Finally, the highest irreversibility of the solar system occurred in the collector with the rate of approximately 79% .

6. ACKNOWLEDGEMENT

The authors would like to acknowledge University of Kurdistan for supporting this research.

REFERENCES

1. Solar Energy, "Renewable Energy Organization of Iran", <http://www.sun.org.ir/fa/sun>.
2. Satcunanathan, S. and Deonarine, S.,
3. "A two pass solar air heater", *Solar Energy*, Vol. 15, (1973), 41–49.
4. Wijesundera, N.E., Lee, A.H. and Tjioe, L.E., "Thermal performance study of two pass solar air heaters", *Solar Energy*, Vol. 28, (1982), 363–370.
5. Persad, P. and Satcunanathan, S., "The thermal performance of the two pass, two glass cover solar air heater", *Solar Energy Engineering*, Vol. 105, No. 3, (1983), 254-258.
6. Moumami, N., Ali, S.Y., Moumami, A. and Desmons, J.Y., "Energy analysis of a solar air collector with rows of fins", *Renewable Energy*, Vol. 29, No.13, (2004), 2053–2064.
7. Mohamad, AA., "High efficiency solar air heater", *Solar Energy*, Vol. 60, No. 2,(1997), 71-76.
8. Sopian, K., Supranto,W.R., Daud, W., Yatim, B. and Othman, M.Y., "Thermal performance of the double-pass solar collector with and without porous media", *Renewable Energy*, Vol. 18, No. 4, (1999), 557–564.
9. Krishnananth, S.S. and Kalidasa Murugavel, K., "Experimental study on double pass solar air heater with thermal energy storage", *Journal of King Saud University –Engineering Sciences*, Vol. 25, No.2, (2013), 135–140.
10. Mahmud Alkilani, M., Sopian, K., Alghoul, M.A., ohif, M. and Ruslan, M.H., "Review of solar air collectors with thermal storage units", *Renewable Sustainable Energy Reviews*, Vol. 15, No. 3, (2011), 1476-1490.
11. Ong, K.S., "Thermal performance of solar air heaters–mathematical model and solution procedure", *Solar Energy*, Vol. 55, No. 2, (1995), 93–109.
12. Mihalakakou,G., "On the use of sunspace for space heating/cooling in Europe", *Renewable Energy*, Vol. 26, No. 3, (2002), 415–429.
13. Ji, J., Luo, C.L., Sun, W., He, W., Pei, G. and Han, C.W., "A numerical and experimental study of a dual-function solar collector integrated with building in passive space heating mode", *Chinese Science Bulletin*, Vol.55, No. 15, (2010), 1568–1573.

14. Zhao, D.L., Li, Y., Dai, Y.J. and Wang, R.Z., "Optimal study of a solar air heating system with pebble bed energy storage", *Energy Conversion and Management*, Vol. 52, No. 6, (2011), 2392–2400.
15. Saadatian, O., Sopian, K., Lim, C.H., Asim, N. and Sulaiman, M.Y., "Trombe walls: a review of opportunities and challenges in research and development", *Renewable & Sustainable Energy Reviews*, Vol. 16, No. 8, (2012), 6340–6351.
16. Carlos, J.S., Corvacho, H., Silva, P.D. and Castro-Gomes, J.P., "Heat recovery versus solar collection in a ventilated double window", *Applied Thermal Engineering*, Vol. 37, (2012), 258–266.
17. John, A.D. and William, A.B., "Solar engineering of thermal processes", Wiley, Hoboken NJ, (2006).
18. Zhang, X.L., Atten, A. and Shen, L.Y., "Green property development practice in China: costs and barriers", *Building and Environment*, Vol. 46, No. 11, (2011), 2153–2160.
19. Bansal, N.K., "Solar air heater applications in India", *Renewable Energy*, Vol. 16, No. 1-4, (1999), 618 – 623.
20. Szargut, J., Morris, D. R. and Stewart, F. R., "Exergy Analysis of Thermal, Chemical and Metallurgical Processes", USA, Edwards Brothers Inc., (1998).
21. Rosen, M.A. and Dincer, I., "Exergy methods for assessing and comparing thermal storage systems", *International Journal of Energy Research*, Vol. 27, No. 4, (2003), 415–430.
22. Akpınar, E.K. and Koçyiğit, F., "Energy and exergy analysis of a new flat-plate solar air heater having different obstacles on absorber plates", *Applied Energy*, Vol. 87, No. 11, (2010), 3438–3450.
23. Bouadila, S., Lazaar, M., Skouri, S., Kooli, S. and Farhat, A., "Energy and exergy analysis of a new solar air heater with latent storage energy", *International Journal of Hydrogen Energy*, Vol. 39, No. 27, (2014), 15266–15274.
24. Gunerhan, H. and Hepbasli, A., "Exergetic modeling and performance evaluation of solar water heating systems for building applications", *Energy and Buildings*, Vol. 39, (2007), 509–516.
25. Bayrak, F., Oztop, H.F. and Hepbasli, A., "Energy and exergy analyses of porous baffles inserted solar air heaters for building applications", *Energy and Buildings*, Vol. 57, (2013), 338–345.
26. Chamoli, S., Chauhan, R., Thakur, N.S. and Sain, J.S., "A review of the performance of double pass solar air heater", *Renewable and Sustainable Energy Reviews*, Vol. 16, (2012), 481–492.
27. Sopian, K., Yigit, K.S., Liu, H.T., Kaka, S. and Vezioglu, T.N., "Performance analysis of photovoltaic thermal air heaters", *Energy conversion and management*, Vol. 37, No. 11, (1996), 1657-1670.
28. Duffie, J.A. and Beckman, W.A., "Solar Engineering and Thermal Processes", New York, Wiley Interscience, (1991).
29. Singh, N., Kaushik, S.C. and Misra, R.D., "Exergetic analysis of a solar thermal power system", *Renewable Energy*, Vol. 19, (2000), 135–143.
30. Petela, R., "Exergy of undiluted thermal radiation", *Solar Energy*, Vol. 74, (2003), 469–488.
31. Tabatabaee, M.H., "Construction installation calculation", Tehran, Kelid Amoozesh, (2008). (In Persian)
32. Sopian, K., Supranto, K., Daud, W.R.W., Othman, M.Y. and Yatim, B., "Thermal performance of double-pass solar collector with and without porous media", *Renewable energy*, Vol. 18, (1999) 557–564.
33. Naphon, P., "Effect of porous media on the performance of the double-pass flat plate solar air heater", *International Communications in Heat and Mass Transfer*, Vol. 32, No. 1-2, (2005), 140 – 150.